International Journal of Pharmaceutics 408 (2011) 173–182

Contents lists available at ScienceDirect

International Journal of Pharmaceutics

journal homepage: www.elsevier.com/locate/ijpharm

Pharmaceutical Nanotechnology

# A novel truncated basic fibroblast growth factor fragment-conjugated poly (ethylene glycol)-cholesterol amphiphilic polymeric drug delivery system for targeting to the FGFR-overexpressing tumor cells

Lulu Cai[a,1], Neng Qiu[a,1], Xia Li[a], Kaili Luo[a], Xiang Chen[a], Li Yang[a], Gu He[a,**], Yuquan Wei[a], Lijuan Chen[a,b,*]

[a] State Key Laboratory of Biotherapy, West China Hospital, West China Medical School, Sichuan University, Chengdu, Sichuan, People's Republic of China
[b] State Key Laboratory Breeding Base of Systematic research, development and Utilization of Chinese Medicine, Chengdu University of Traditional Chinese Medicine, Chengdu, Sichuan, People's Republic of China

ARTICLE INFO

*Article history:*
Received 12 October 2010
Received in revised form 18 January 2011
Accepted 21 January 2011
Available online 26 January 2011

*Keywords:*
Tumor-targeting drug delivery
Chol-PEG$_{2000}$-COOH polymer
truncated bFGF-conjugated micelles
paclitaxel

ABSTRACT

Targeted uptake of therapeutic nanoparticles in tumor cells-specific manner represents a potentially powerful technology in cancer therapy. In present study, we proposed a drug delivery system formulated with biocompatible and biodegradable cholesterol-block-poly (ethylene glycol) (Chol-PEG$_{2000}$-COOH) polymer. And the surface of the polymer was chemically linked with truncated bFGF fragments (tbFGF). The tbFGF could recognize fibroblast growth factor receptors (FGFR) that are highly expressed by a variety of human cancer cells. The micelles had a size distribution of about 10–50 nm and significantly enhanced the cytotoxicity of paclitaxel to LL/2 cells as demonstrated by MTT test ($IC_{50}$ = 0.21 μg/mL for tbFGF conjugated Chol-PEG$_{2000}$-COOH micelles (tbFGF-M-PTX) versus 26.43 μg/mL for free paclitaxel, respectively). Flow cytometry revealed the cellular uptake of rhodamine B encapsulated in the tbFGF-conjugated micelles was increased by 6.6-fold for HepG2, 6.2-fold for A549, 2.9-fold for C26 and 2.7-fold for LL/2 tumor cells, respectively, compared with micelles without tbFGF. The fluorescence spectroscopy images further demonstrated that the tbFGF conjugated micelles could specifically bind to the tumor cells that over-expressed FGFRs and then release rhodamine B into the cytoplasm. Our results suggest the tbFGF conjugated Chol-PEG$_{2000}$-COOH micelles have great potential application for tumor targeting therapy.



## 1. Introduction

One of the central problems in the cancer chemotherapy is the severe toxic side effects of anticancer drugs on normal tissues (Kerbel, 2000; Kong and Crystal, 1998; Shchors and Evan, 2007; Zamboni, 2005). Typical chemotherapeutic agents have low water solubility, short blood half-lives, narrow therapeutic indices, and high systemic toxicity (Sutton et al., 2007). To reduce the side effects of these drugs on normal organs, tumor-targeting drug delivery systems have been developed. In recent years, various nanocarriers including liposome, nanoparticle and micelle have been reported to improve the insolubility of chemotherapeutic agents, prolong their half-lives *in vivo*, minimize the uptake of the drug by normal cells and enhance the influx and retention of the drug in tumor cells to achieve the most antitumor efficacy and the least system toxicity (Lee et al., 2007; Sutton et al., 2007; Zamboni, 2005).

Polymeric micelles have recently emerged as a powerful nanomedicine platform for cancer therapeutic applications (Lasic, 1992; Lee et al., 2007; Sutton et al., 2007). These micelles have the particle size in the range of 10–100 nm, and can solubilize hydrophobic drugs through hydrophobic interactions and/or hydrogen bonds, while expose their hydrophilic shells to the external environment. These functions effectively protect the entrapped bioactive drugs from degradation and enable them to exhibit prolonged activity in the systemic circulation by avoiding the scav-

*Abbreviations:* tbFGF, the truncated basic fibroblast growth factor; FGFR, the fibroblast growth factor receptors; Chol-PEG$_{2000}$-COOH, the cholesterol-block-poly (ethylene glycol) copolymer; PTX, the paclitaxel; tbFGF-M-PTX, the paclitaxel encapsulated tbFGF conjugated Chol-PEG$_{2000}$-COOH micelles; M-PTX, the paclitaxel encapsulated Chol-PEG$_{2000}$-COOH micelles without tbFGF; tbFGF-M-RB, the rhodamine B-loaded Chol-PEG$_{2000}$-COOH micelles conjugated with the tbFGF fragments; M-RB, the rhodamine B-loaded Chol-PEG$_{2000}$-COOH micelles without the tbFGF fragments; AFM, the atomicforce microscopy; TEM, the transmission electron microscope.

* Corresponding author at: State Key Laboratory of Biotherapy, West China Hospital, Sichuan University, 4 Keyuan Road, 1 Gaopeng Street, Chengdu 610041, Sichuan, People's Republic of China. Tel.: +86 28 85164103; fax: +86 28 85164060.
** Corresponding author. Tel: +86 28 85164103; fax: +86 28 85164060.
*E-mail addresses:* hegu@scu.edu.cn (G. He), lijuan17@hotmail.com (L. Chen).
[1] These authors equally contributed to this paper.

0378-5173/$ – see front matter © 2011 Elsevier B.V. All rights reserved.
doi:10.1016/j.ijpharm.2011.01.042

enging of the reticuloendothelial systems (RES) (Liu et al., 2008). Although the initial anti-tumor efficacy of these systems seems promising, significant micelle uptake by reticuloendothelial systems such as liver and spleen has also been observed. To further improve the delivery efficiency and cancer specificity, a strong research impetus has been placed on micelle functionalization in order to achieve tumor targeting and site-specific drug release, with the hope of reaching a more pronounced tumor response (Sutton et al., 2007; Yamamoto et al., 2001). In recent years, Torchilin et al. have reported that the monoclonal antibody (mAb)-modified PEG-PE micelles could recognize and bind to numerous tumor cells but not normal cells *in vitro* (Torchilin et al., 2003). Yang et al. have developed a TAT-PEG-Chol micelle which could cross the blood-brain barrier and locate around the cell nucleus of neurons (Liu et al., 2008). Dharap et al. have reported that the micelle of CPT-PEG-LHRH conjugates substantially enhance the efficacy of chemotherapy, which lead to amplify apoptosis induction in the tumor, and minimize the side effects of the anticancer drug on normal organs (Dharap et al., 2005). These micelles modified with antibodies or peptides enhance the cellular uptake of loaded drugs by targeting to the tumor cells actively.

Fibroblast growth factors (FGFs) are small peptide growth factors and play important roles in tumor growth and angiogenesis because of their high affinity to heparin (Goldman et al., 1997; Rancourt et al., 1998; Sosnowski et al., 1996). Fibroblast growth factor receptors (FGFRs) are found to be ubiquitously upregulated in numerous tumor cells and on tumor neovasculature *in situ*, in comparison to normal tissues (Li et al., 2007). Thereby, FGFRs have become potential targets for drug delivery and cancer therapy. In a previous report, the peptide KRTGQYKLC (bFGFp) could interact with FGFR1 via binding to bFGF, and is useful as a targeting ligand for tumor cells (Terada et al., 2006). Polyethylene glycol (PEG)-grafted bFGFp-liposomes has been reported to be a potential targeting approach to reduce nonspecific binding (Harashima et al., 2002). Terada et al. have reported that 10% $mPEG_{3000}$/bFGFp-liposomes produced a significant increase in the uptake by NIH3T3, A549, and BL6 cells with high expression of FGFR, but no increase in CHO-K1 cells without expression of FGFR (Terada et al., 2007).

In our previous study, we constructed a truncated human bFGF (tbFGF) peptide (a.a. 30–115), which contains bFGF receptor binding site and a part of heparin-binding site. This tbFGF peptide can effectively bind to FGFRs on cell surface, but not stimulate cell proliferation (He et al., 2003). Using this tbFGF peptide, we have developed FGFRs-mediated cationic liposomes to target doxorubicin or paclitaxel to FGFRs-overexpressed tumor cells and tumor neovasculature endothelial cells *in vitro* and *in vivo*. Such delivery systems not only improve the uptake of chemotherapeutic agents in tumor and HUVEC cells, but also showe significant inhibition of tumor growth and improvement of survival of tumor-bearing mice (Chen et al., 2010). In this work, the tbFGF conjugated Chol-$PEG_{2000}$-COOH micelle is chosen as a delivery system of chemotherapeutic agents for increasing the aqueous solubility and cytoxicity of the drugs, and more importantly, achieving tumor cell targeting and specific drug uptake. Firstly, the Chol-$PEG_{2000}$-COOH block polymer is synthesized for the purpose of forming sterically stabilized micelles. And then the paclitaxel or rodanmin B loaded Chol-$PEG_{2000}$-COOH micelles are formed through the solvent evaporation method. Finally, the truncated fibroblast growth factor fragments (tbFGF) are conjugated to the carboxyl terminals of Chol-$PEG_{2000}$-COOH on the surface of the micelles. This self-assembled tbFGF-conjugated Chol-$PEG_{2000}$-COOH micelle has a hydrophobic core of cholesterol for drug incorporation and a hydrophilic shell of PEG with stable conjunction of tbFGF. Hence, this novel tumor targeting drug delivery system may have several functions for tumor therapy: 1) the Chol-$PEG_{2000}$-COOH micelles could provide prolonged drug effects because of their sustained release characteristic, and protect the encapsulated agent from enzymatic degradation; 2) the small size(10-50 nm) of the micelles would improve the penetration, accumulation, and antitumor activity of chemotherapeutic drug by enhancing the permeability and retention (EPR) effect; 3) the tbFGF could specifically target to the tumor cells by binding with the FGFRs, resulting in special uptake of antitumor drugs.

## 2. Material and methods

### 2.1. Chemicals

Poly (ethylene glycol) (PEG, Mr = 2000) and cholesterol were purchased from Sigma (USA). Paclitaxel was purchased from Chengdu Mansite Pharmaceutical Co. Ltd. Rhodamine B was purchased from Fluka (UK). 1-(3-Dimethylaminopropyl)-3-ethylcarbodiimide hydrochloride (EDC), and N-Hydroxysuccinimide (NHS) were purchased from Chengdu Kelong Chemical Co. Ltd. DMEM, RPMI-1640 and 3-(4,5-dimethylthiazol -2-yl)-2,5-diphenyl tetrazolium bromide (MTT) were purchased from Sigma (USA). All the chemicals used in this work were analytical pure grade.

### 2.2. Cell cultures

The human lung cancer cell lines A549, murine cancer cell lines LL/2, human hepatocellular liver carcinoma cell lines HepG2 and murine colorectal cancer cell lines C26 were purchased from American Type Culture Collection (ATCC; Manassas, VA). A549 cells were incubated in RPMI-1640 medium (GIBICO). LL/2, HepG2 and C26 cells were incubated in DMEM medium (GIBICO). These cells were supplemented with 10% heat-inactivated fetal calf serum, 100 units/mL penicillin, 100 units/mL streptomycin, and incubated at 37 °C, 95% relative humidity, under 5% $CO_2$. The concentration of cells was determined by counting trypsinized cells with a hemocytometer.

### 2.3. Preparation of bFGF fragment

The truncated bFGF (tbFGF) peptide (a.a.30-115), containing bFGF receptor binding site and a part of heparin-binding site, can effectively bind to FGFRs on cell surface, but not stimulate cell proliferation. The sequences of tbFGF are KRLYCKNGGFFLRIHPDG-RVDGVREKSDPHIKLQL-QAEERGVVSIKGVCANRYLAMKEDGRLLAS-KCVTDECFFFERLESNNYNTY (He et al., 2003). The preparation and purification of the truncated bFGF peptides were described in our previous work (He et al., 2003). The purity of recombinant bFGF could be achieved up to 99%. The characterization of tbFGF was confirmed by western blot with anti-bFGF antibody in our previous work (He et al., 2003).

### 2.4. Synthesis of Chol-$PEG_{2000}$-COOH

Cholesterol (7.72 g, 20 mmol), succinic anhydride (4.03 g, 40 mmol), and 4-dimethylaminopyridine (DMAP) (2.44 g, 20 mmol) were dissolved in 100 mL $CH_2Cl_2$. The excess of succinic anhydride was used to guarantee that hydroxy terminals of cholesterol were totally reacted. The mixture was stirred at room temperature for 15 h, until no excess cholesterol was detected on TLC (dichloromethane: methanol: ethyl acetate, 7:1:1).The reaction solution was concentrated by rotary evaporation and then recrystallized twice in glacial acetic acid solution to obtain a white powder of cholesteryl hydrogen succinate.

Synthesis of Chol-PEG2000-OH was carried out according to the method previously reported with some modification. The $PEG_{2000}$ (6.00 g, 3 mmol), cholesterol succinate (0.98 g, 2 mmol), DMAP

(0.25 g, 2 mmol), and DCC (0.83 g, 4 mmol) were dissolved in 50 mL $CH_2Cl_2$. The mixture was stirred at room temperature for 24 h. After removal of the *N*, *N*-dicyclohexylurea precipitates by filtration, the filtrate was concentrated by rotary evaporation, and precipitated in ethylether, and then the white precipitate was collected. The crude product was further purified by silica gel column chromatography using a step gradient of methanol (1–5%) in dichloromethane. The fractions containing Chol-$PEG_{2000}$-OH were collected and then evaporated to dryness under vacuum. A single spot was visualized with iodine vapour by TLC analysis (dichloromethane: methanol, 10:1).

Chol-$PEG_{2000}$-OH (987 mg, 0.4 mmol), succinic anhydride (100 mg, 1 mmol), and DMAP (49 mg, 0.4 mmol) were dissolved in 10 mL $CH_2Cl_2$. Then 300 μL TEA (triethylamine) was added to the reaction. The mixture was heated to reflux. After no Chol-$PEG_{2000}$-OH was detected on TLC (chloroform: methanol, 10:1), the reaction was cooled to room temperature. The $CH_2Cl_2$ solution was washed twice with $^1$N HCl, and then washed twice with water. The organic phases were dried with $MgSO_4$ and then evaporated to obtain Chol-$PEG_{2000}$–COOH as white powder. The $^1$H NMR spectrum of $PEG_{2000}$, Chol-$PEG_{2000}$-OH, and Chol-$PEG_{2000}$-COOH were studied using a Bruker Avance 400 spectrometer (400 MHz), and $D_2O$ was used as the solvent.

### 2.5. Micelle formation and drug loading

The paclitaxel loaded Chol-$PEG_{2000}$-COOH micelles (M-PTX) were prepared as following: 2 mg paclitaxel and 40 mg Chol-$PEG_{2000}$-COOH were dissolved in 4 mL mixed solvent of methanol and chloroform (v/v = 1:1) at room temperature. To form the dry drug-containing lipid film, the solvents were removed on the rotary evaporator. The dried lipid film was hydrated by 2 mL of 10 mM MES buffer (pH 5.0) at 40 °C for 30 min, then sonicated at 40 °C for 5 min. The micelles were extruded through 0.2 μm pore size polycarbonate filter and centrifuged at 3000 rpm for 3 min to remove unloaded drugs. The final concentration of paclitaxel was measured by high-performance liquid chromatography (HPLC) analysis. The rhodamine B ($\lambda_{max}$ = 543 nm) loaded micelles (M-RB) were prepared by the similar method of M-PTX, and the ratio of rhodamine B to Chol-$PEG_{2000}$-COOH were 1 to 10 (w/w). Then unentrapped rhodamine B was removed using Sephadex G-75 chromatography (GE Healthcare, Amersham Biosciences, NJ, USA) (Chen et al., 2010).

### 2.6. Conjugate of tbFGF fragments to the surface of Micelles

To make the surface of micelles functional, tbFGF fragments were conjugated to the carboxyl terminals of Chol-$PEG_{2000}$-COOH with EDC and NHS as accelerants. Briefly, 1 mL of micelle solutions (the Chol-$PEG_{2000}$-COOH concentration was 20 mg/mL in 10 mM MES buffer, pH 5.0) were incubated at 4 °C, then 320 μmol NHS (N-hydroxysuccinimide) and 640 μmol EDC(1-ethyl-3-(3-dimethylaminopropyl)-carbodiimide) were added and stirred for 15 min at room temperature. Then 0.1 M NaOH solutions were added to adjust the pH of the solution to 7.4, which allow for the reaction between the amino-groups of tbFGF fragments and carboxyl groups of Chol-$PEG_{2000}$-COOH. Then 358 μmol tbFGF fragments (2.5 mg/mL) were added to the solution and the reaction was continued at 4 °C overnight with slightly stirring. After this, the unreacted tbFGF fragments, EDC and NHS were removed by dialysis with 10 mM PBS (pH 7.4) for 8 h, using cellulose ester membranes with a cut off size of 250 kDa.

### 2.7. Size and Zeta-potential determination

Particle size and Zeta potential of the micelles conjugated with or without tbFGF fragments were determined by dynamic light scattering (DLS) with a Zetasizer Nano ZS-90 instrument (Malvern Instruments, Malvern, UK). The micelle suspension (the concentration of paclitaxel was 2 mg/mL) was diluted 10 times with de-ionized (DI) water before measurement. Refractive index was 1.330 and temperature was kept at 25 °C during measuring process. All the tests were run 3 times and took mean values.

### 2.8. Atomic force microscopy (AFM) and transmit electronic microscopy (TEM)

The morphology of prepared micelles was observed under an atomic force microscopy (AFM) and a transmission electron microscope (TEM). AFM images were taken by tapping mode in air on an atomic force microscopy (SPA400, Seiko, Japan). The prepared micelle suspension was diluted with de-ionized (DI) water and deposited onto freshly cleaved mica lamella. The sample was dried for 3 h at room temperature. For TEM, micelles were diluted with distilled water and placed on a copper grid covered with nitrocellulose. The sample was negatively stained with phosphotungstic acid and dried at room temperature, after which TFM images were taken by a transmission electron microscope(H-6009IV, Hitachi, Japan)

### 2.9. SDS-PAGE protein electrophoresis and protein assay

12% Sodium dodecyl sulfate polyacrylamide gel (SDS-PAGE) was used for protein electrophoresis to determine whether tbFGF fragments were attached to the surface of micelles (Zelphati et al., 2001). The paclitaxel loaded Chol-$PEG_{2000}$-COOH micelles with tbFGF (tbFGF-M-PTX) were developed by the above-mentioned method. Control of free tbFGF peptide went through the same chemical condition as the synthesis process of the tbFGF-M-PTX. Then 25 μL samples of tbFGF-M-PTX, the physical mixture of M-PTX and tbFGF, and Control with 5 μL loading buffer were loaded onto 8 cm × 10 cm SDS-PAGE. After running at 80 mV for 15 min and 120 mV for 35 min, the gel was stained in 0.25% Coomassie Blue solution (methanol: acetic acid: water = 30:10:60, v/v/v) and destained in methanol: acetic acid: water (30:10:60, v/v/v) and then destained in methanol: acetic acid: water (30:10:60, v/v/v). The amount of tbFGF peptide bound onto micelles' surface was quantified by the Micro BCA method. In brief, 500 μL Micro BCA working solution was added to 500 μL tbFGF-M-PTX and M-PTX (served as control), respectively. After 60 min of incubation, the absorbance was measured at 562 nm using a spectrophotometer (Molecular Devices, Sunnyvale, USA). The results were compared to a standard curve of tbFGF peptide solution ranged from 0.5 μg/mL to 20 μg/mL.

### 2.10. In vitro drug release

The release profile of paclitaxel from micelles was investigated at pH 7.4 using the dialysis method. Briefly, the drug loaded micelle solution was placed in a dialysis bag (molecular weight cut off = 8 kDa) suspended in 0.5 L of PBS (pH 7.4, 0.01 M) in 37 °C water bath with slightly shaking. At given time points, 1 mL buffer was taken from the incubated medium and quantified the content of paclitaxel by high-performance liquid chromatography (HPLC) assay.

### 2.11. Cytotoxicity assay

Cell cytotoxicity of blank micelles, free paclitaxel, paclitaxel loaded micelles(M-PTX) or tbFGF conjugated M-PTX (tbFGF-M-PTX) were evaluated by MTT (3-[4,5-dimethylthiazol-2-yl]-2,5-diphenyl tetrazolium bromide) assay using murine Lewis lung cancer cell lines LL/2. Samples containing $1 \times 10^4$ cells in 100 μL DMEM containing 10% FBS were plated in 96-well plates and incu-

bated for 24 h at 37 °C in humanized atmosphere containing 5% $CO_2$. These cells were incubated with different concentration solutions of blank micelles, free paclitaxel, M-PTX or tbFGF-M-PTX for 48 h in same condition. After incubation, 20 μL MTT (5 mg/mL, dissolved in PBS, pH 7.4) was added to each well and incubated for another 4 h. Then removed the incubated medium, added 150 μL DMSO to each well and gently shook for 10 min at room temperature. Absorbance was measured at 570 nm using a Spectramax M5 Microtiter Plate Luminometer (Molecular Devices, US). Set the absorbance value of untreated cells to be 100%. The concentration of paclitaxel at which inhibited 50% cell growth compared with untreated cells ($IC_{50}$) was defined by curve fitting (LOGIT method) using SPSS software. Each experiment was repeated three times in triplicate ($n = 9$).

### 2.12. Cellular binding and uptake study

The cellular uptake tests of Chol-$PEG_{2000}$-COOH micelles with and without tbFGF fragments were performed in various cell lines (including LL/2, A549, HepG2, and C26) by microscope and flow cytometric assay. $3 \times 10^5$ cells were placed in each well of 6-well plates and grown for 24 h in 2 mL DMEM medium (A549 were incubated in RPMI-1640 medium) supplemented with 10% fetal bovine serum (FBS), penicillin (100 U/mL), and streptomycin (100 U/mL) at 37 °C in 5% $CO_2$. Micelles conjugated with or without tbFGF fragments loading with 2 μg rhodamine B were added to predesigned wells and incubated for 3 h at 37 °C in 5% $CO_2$. After incubation, growth media in the wells was removed, and the cells were washed with physiological saline for 3 times. Fluorescence and light microscope (Olympus IX71, Olympus, Japan) were used to observe the fluorescence from rhodamine B that entered into the tumor cells. Then collected the cells and a flow cytometer (EPICS Elite ESP, Beckman Coulter, US) was used to detect the fluorescence from individual cells. For detection of the fluorescence from rhodamine B, an excitation light of 488 nm was achieved with argon laser, and emission fluorescence was between 564 and 606 nm.

### 2.13. Intracellular distribution study

A cellular distribution study was performed by fluorescence microscopy. Briefly, A549 and C26 cells were seeded on glass coverslips in 6-well plates at a density of $1 \times 10^5$ cells/well. After complete adhesion, the cells were washed 2 times with growth media and incubated at 37 °C in 5% $CO_2$ for 1 h with the rhodamine B-loaded micelles conjugated with the tbFGF fragments (tbFGF-M-RB). The tbFGF fragments were pre-labeled with FLUOS using a Protein Fluorescence Label Kit (Roche, Basel, Switzerland). After incubation, the micelle solution was removed, and the cells were washed 3 times with physiological saline, followed by fixation with 1% paraformaldehyde (PFA) for 10 min. Thereafter, cells were incubated with Hoechst 33258 for 30 min to visualize the nucleus. Finally, images of FLUOS, rhodamine B and Hoechst 33258 were obtained by fluorescence microscope (Olympus IX71, Olympus, Japan).

### 2.14. Statistics

Statistical significance between pairs of samples was measured using the 2-tailed Student's *t*–test. Data were considered significant at $p < 0.05$.

## 3. Results

### 3.1. Synthesis and identification of Chol-$PEG_{2000}$-COOH

The synthesis of Chol-$PEG_{2000}$-COOH was according to the literatures with some modifications (Bikram et al., 2004; Rosa et al., 2007). Carboxylic-terminated Chol-$PEG_{2000}$ was directly attached to cholesterol at one end of PEG diacid, which was prepared by functionalization of $PEG_{2000}$ with disuccnic acid or diglutaric acid. The main disadvantage of coupling one cholesterol molecular at one end of PEG is the poor selectivity of PEG diacid which results in low yield and purity of Chol-$PEG_{2000}$-COOH. To avoid this problem, Chol-$PEG_{2000}$-COOH was synthesized by reacting succinic anhydride with Chol-$PEG_{2000}$-OH. The cholesterol was firstly reacted with excess succinic anhydride and the crude product was purified in glacial acetic acid. The resulting cholesterol succinate derivative was then reacted with the PEG in the presence of DCC and DMAP. The molar number of the PEG was 1.5-fold of the cholesterol succinate derivative and ensures a high yield of Chol-$PEG_{2000}$-OH. After purified by gradient elution column chromatography, the product was reacted with succinic anhydride and the Chol-$PEG_{2000}$-COOH was finally obtained.

Fig. 1(A) represents the synthesis procedure of the Chol-$PEG_{2000}$-COOH conjugate. $^1$H NMR spectrum of Chol-$PEG_{2000}$-COOH demonstrated the successful synthesis of Chol-$PEG_{2000}$-COOH. As shown in Fig. 1(B), the multiplet at δ3.47-3.76 was attributed to the repeating units in PEG, and the six- and three-position protons in cholesterol were found at 5.36 ppm and 4.59 ppm, respectively. Signals at 4.24 ppm were assigned to the methylene protons in PEG adjacent to the succinyl group which appeared upon the reaction, and the peaks at 2.70 were attributed to the methylene proton of succinyl group (–$CH_2$–C=O), while the peaks appearing at 2.33 were assigned to the four position of the cholesterol. All of the other multiple signals at

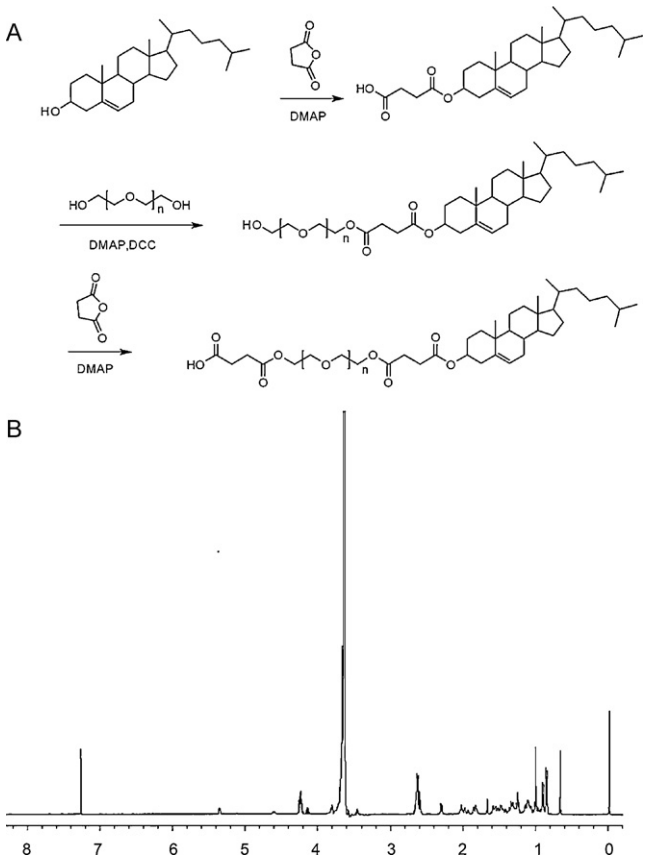


**Fig. 1.** Synthesis and identification of the Chol-$PEG_{2000}$-COOH copolymers. A: the chemical reaction scheme for preparing the Chol-$PEG_{2000}$-COOH conjugate. B: the $^1$H NMR spectra of Chol-$PEG_{2000}$-COOH in $D_2O$.

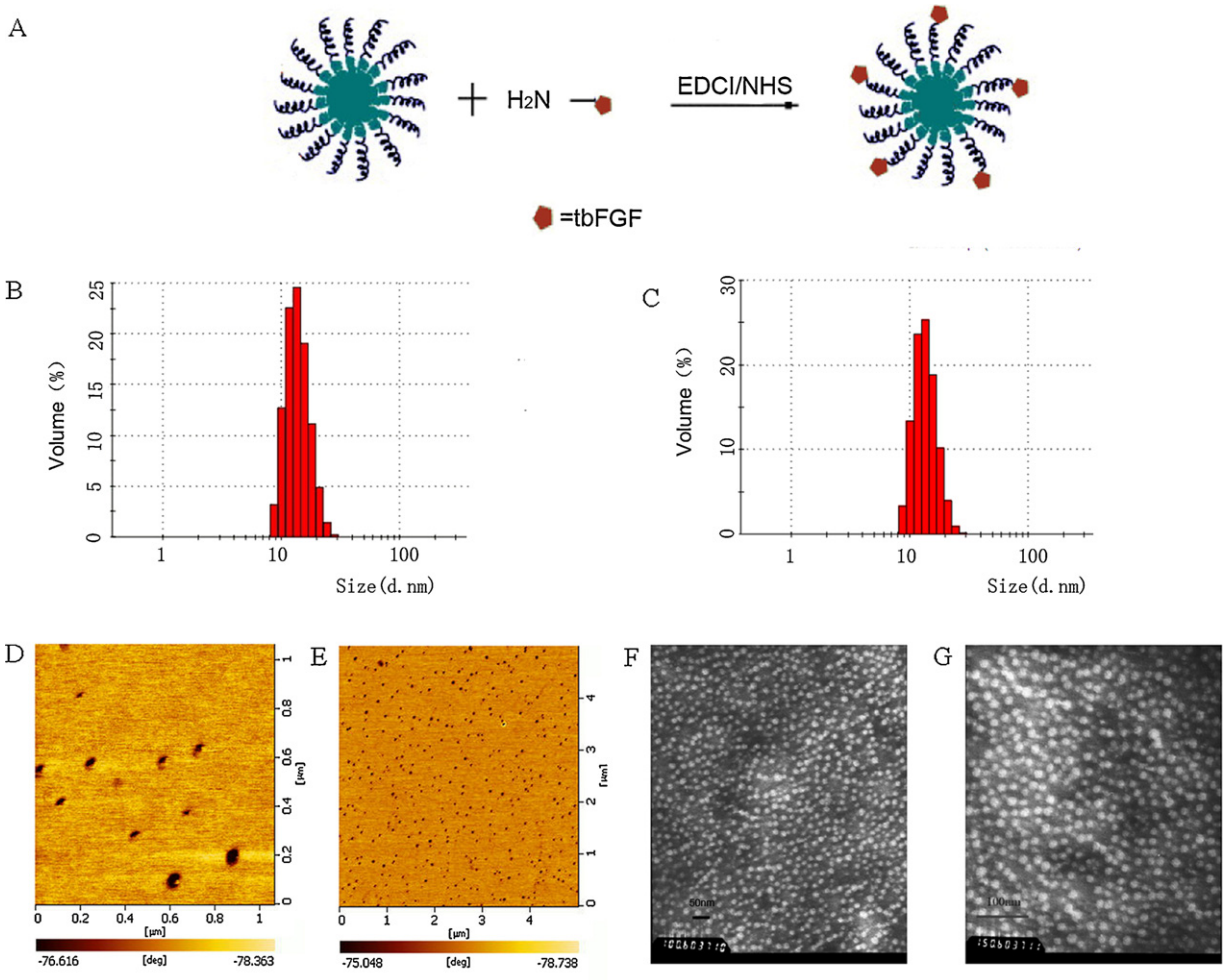


**Fig. 2.** Preparation and characterization of the paclitaxel loaded tbFGF-conjugated Chol-$PEG_{2000}$-COOH micelles. A: Diagram of the preparation of tbFGF-conjugated Chol-$PEG_{2000}$-COOH micelles. B: Size distribution of the paclitaxel loaded Chol-$PEG_{2000}$-COOH micelles (M-PTX). C: Size distribution of the paclitaxel loaded tbFGF-conjugated Chol-$PEG_{2000}$-COOH micelles (tbFGF-M-PTX). D and E: typical AFM images of tbFGF-M-PTX (size of the scale bar: 1 um for D and 5 um for E). F and G: typical TEM images of tbFGF-M-PTX (size of the scale bar: 50 nm for F and 100 nm for G).

0.68–2.05 came from the protons in cholesterol. These results further demonstrated that the conjugate had been successfully prepared.

### 3.2. Characterization of paclitaxel loaded Chol-$PEG_{2000}$-COOH micelles with or without tbFGF fragment modification

In our study, the mean size of paclitaxel loaded micelles was $30.86 \pm 2.91$ nm (mean ± SD; $n = 3$) with a distribution from 8.72 nm to 42.67 nm (PDI = 0.26) (Fig. 2B). The dynamic light scattering (DLS) data also showed that the micelles size ($36.82 \pm 1.20$ nm, PDI = 0.29, mean ± SD; $n = 3$) did not increase obviously ($P > 0.05$) after attachment of tbFGF fragment (Fig. 2C). Further atom force microscopy and transmit electronic microscopy analyses confirmed that the micelles conjugated with tbFGF fragment were spheroids with regular shape and a size distribution of 10–45 nm (Fig. 2D–G). The HPLC results showed that the micellar PTX loading efficiency was >90% (Date not shown). Zeta potential measurement showed that the surface charges of M-PTX and tbFGF-M-PTX were $-5.47 \pm 0.91$ mV (mean ± SD; $n = 3$) and $-1.60 \pm 0.18$ Mv (mean ± SD; $n = 3$) respectively (pH 7.4). Because the isoelectric point of tbFGF fragments is pH 8.77, the increase of zeta potential of tbFGF-M-PTX (compared to M-PTX) ($p < 0.05$) might contribute to the positive charge of the tbFGF fragments which were bound to the surface of micelles (pH 7.4).

### 3.3. Determination of tbFGF peptides on the surface of M-PTX

To confirm whether tbFGF fragments were bound to the surface of micelles, a SDS-PAGE protein electrophoresis test was performed. As shown in Fig. 3A, the band of free tbFGF fragments (a) was slightly stronger than that of the mixtures of protein and micelle (b). The slight decrease of the band of protein-micelle physical mixtures is presumably due to the electrostatic combination of tbFGF fragments and micelles which made the tbFGF to be captured by the micelles and shifted. However the binding efficiency by electrostatic force was not ideal. In contrast, when tbFGF fragments were chemically combined with micelles, the protein band almost disappeared, indicating that most of tbFGF fragments were attached to the surface of micelles(c). The quantitive protein assay indicated that the amount of tbFGF conjugated on the surface of micelles was approximately $32.1 \pm 2.6$ μg tbFGF/mg Chol-$PEG_{2000}$-COOH (mean ± SD; $n = 3$).

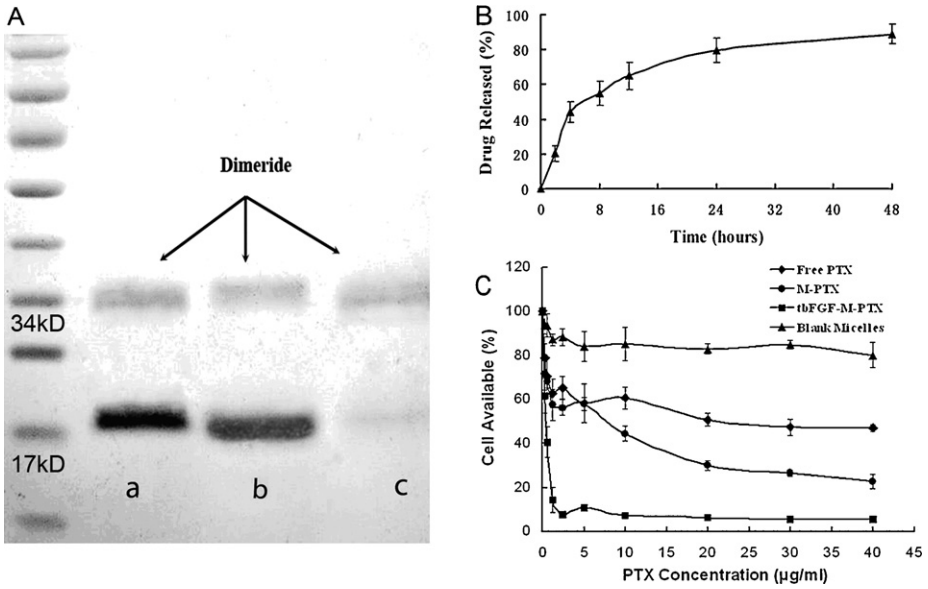


**Fig. 3.** Micelle-tbFGF conjunction efficiency, release profile and cytotoxic effect of the tbFGF-M-PTX *in vitro*. A: SDS-PAGE electrophoresis assay of free tbFGF fragments which have gone through the same chemical condition as the synthesis process of tbFGF-M-PTX (a), the mixture of tbFGF and M-PTX (b) and the tbFGF-M-PTX(c) to determine whether tbFGF fragments were bound to the surfaces of Chol-$PEG_{2000}$-COOH micelles. B: Time course of paclitaxel releasing from tbFGF-M-PTX at 37 °C and pH 7.0. Released paclitaxel was separated from tbFGF-M-PTX by dialysis and quantified using HPLC(Error bars correspond to 95% confidence intervals). C: Cytotoxicity of the soluble form of free PTX (□), blank micelles (▲), M-PTX (●) and tbFGF-M-PTX (■) on LL/2 cell lines. The percentage of viable cells was quantified using the methylthiazoletetrazolium method. Mean values and 95% confidence intervals derived from three independent experiments are shown. $P < 0.05$.

### 3.4. *In vitro release profile of paclitaxel from tbFGF-M-PTX*

The *in vitro* release profile of paclitaxel from tbFGF fragment conjugated Chol-$PEG_{2000}$-COOH micelles (tbFGF-M-PTX) was studied at 37 °C and pH 7.0. Data suggests that paclitaxel can be well encapsulated in Chol-$PEG_{2000}$-COOH micelles, and released in an extended period. As shown in Fig. 3B, approximate 54% of total drug released after 8 h, followed by release of 89% in 48 h.

### 3.5. *Cell cytotoxicity of micelle-encapsulated paclitaxel*

To evaluate the cytotoxicity enhancement by paclitaxel encapsulated in tbFGF-M-PTX, 3-[4,5-dimethylthiazol-2-yl]-2, 5-diphenyl tetrazolium bro-mide (MTT) assay was used. After 48 h incubation with the soluble form of free PTX, balnk micelles, M-PTX or tbFGF-M-PTX, cytotoxicity was measured following the absorbance of the degraded MTT at 570 nm. As shown in Fig. 3C, tbFGF-M-PTX showed significantly higher cytotoxicity than free paclitaxel or M-PTX. The mean concentrations of paclitaxel that caused 50% cell inhibition (IC50) of tbFGF-M-PTX was decreased to 0.21 μg/mL compared with 26.43 μg/mL of free paclitaxel and 3.85 μg/mL of M-PTX, respectively. The tbFGF-M-PTX revealed 150-fold and 18-fold increase of cytotoxicity in comparison to free PTX and M-PTX, respectively ($p < 0.05$).The blank micelles did not show apparent cytotoxicity to LL/2.

### 3.6. *Cell uptake and binding study of tbFGF fragment conjugated micelles*

To evaluate whether tbFGF fragments could increase drug uptake by tumor cells that overexpress FGFRs, LL/2, A549, HepG2 and C26 cells were treated with micelles encapsulated with rhodamine B. After incubation for specific time, the cells were washed, then identified using a fluorescence or light microscopy and collected for analysis of rhodamine B-derived fluorescence by flow cytometry. The flow cytometry data (Fig. 4A) shows the distri-

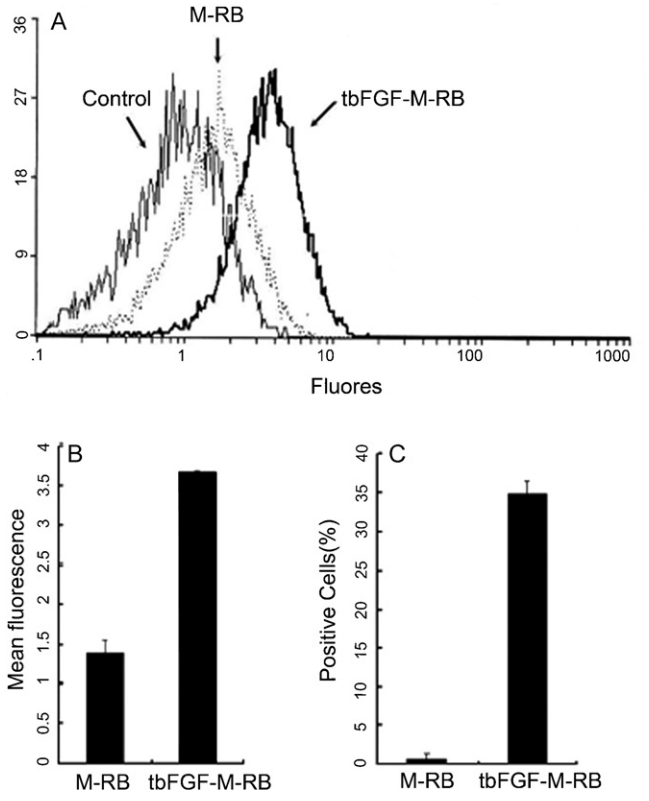


**Fig. 4.** Different cellular uptake of rhodamine B loading micelles with or without tbFGF by LL/2 cells. A: Intracellular rhodamine B fluorescence intensities in LL/2 cells after incubation with tbFGF-M-RB, M-RB or empty Chol-$PEG_{2000}$-COOH micelles (Control); B: Quantification of the mean fluorescence intensities of intracellular rhodamine B from M-RB or tbFGF-M-RB, respectively; C: The percentage of positive cells which contained rhodamine B after incubated with M-RB or tbFGF-M-RB, respectively. Error bars correspond to 95% confidence intervals. $P < 0.05$.

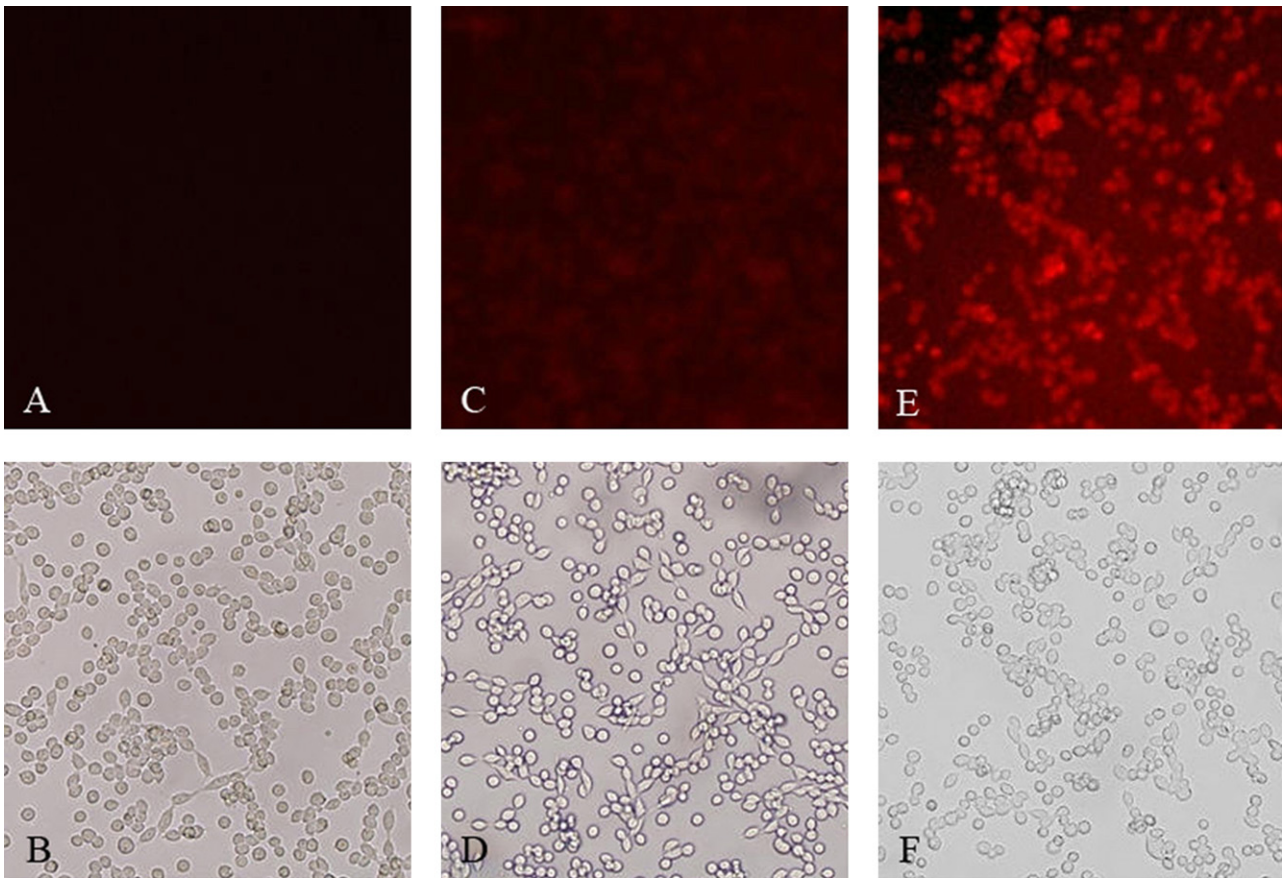


**Fig. 5.** The fluorescence microscopy images and white light microscopy images of LL/2 cells after incubation with different rhodamine B loaded micelles: Control (A and B); the M-RB (C and D); the tbFGF-M-RB (E and F).

bution of intensity in LL/2 cells treated with tbFGF-M-RB, M-RB or empty Chol-$PEG_{2000}$-COOH micelles (Control). The mean fluorescence intensity of rhodamine B uptaken by cells treated with tbFGF-M-RB was increased by 2.67-fold (mean = 3.68 *vs.* 1.38 arbitrary units, $p < 0.05$) compared with that treated with M-RB (Fig. 4B). The percentage of positive cells containing rhodamine B after incubated with tbFGF-M-RB was significantly increased by 36.63-fold (mean = 34.8% *vs.* 0.95%, $p < 0.05$) in comparison to that incubated with M-RB (Fig. 4C). These results indicate that the tbFGF fragments on the surface of micelles indeed enhanced the uptake of the drug (rhodamine B) by tumor cells. which were further confirmed by the fluorescence and white light microscopy images(Fig. 5). Fig. 5.clearly shows that tbFGF-M-RB could effectively entry LL/2 tumor cells, while no rhodamine was detected in cells that incubated with M-RM. To further confirm the selectivity of tbFGF-M-RB to tumor cells, A549, HepG2 and C26 cells incubated with tbFGF-M-RB or M-RB were determined by flow cytometry, too. As shown in Fig. 6, the cells incubated with tbFGF-M-RB showed markedly higher fluorescence intensity than that with M-RB both in A549 cells and HepG2 cells. The mean fluorescence intensity of tbFGF-M-RB were increased by 6.6-fold (mean = 31.5 *vs.* 4.8 arbitrary units, $p < 0.05$) in HepG2 and 6.2-fold (mean = 18.6 *vs.* 3.0 arbitrary units, $p < 0.05$) in A549 compared with M-RB. For C26 cells, although the expression of FGFRs was limited, the cellular uptake of tbFGF-M-RB was still 2.9-fold higher than that of M-RB (mean = 3.63 *vs.* 1.25 arbitrary units, $p < 0.05$), which suggests that the cellular binding and uptake of the tbFGF-M-RB are mostly induced by the recognition of the tbFGF fragments and the FGFRs.

### *3.7. Intracellular distribution of tbFGF-M-RB by visualized triple fluorescence-labeling experiments*

To determine the intracellular distribution of tbFGF-M-RB more precisely, we performed triple fluorescence-labeling experiments and visualized blue fluorescence from Hoechst 33258, red fluorescence from rhodamine B and green fluorescence from FLUOS-labeled tbFGF fragments after predetermined treatment time. As shown in the Fig. 7, although the treatment time of micelles was only 1 h, the green fluorescence from FLUOS-labeled tbFGF fragments (A and D) were detected on the surfaces of most cells (A–C for A549 and D–F for C26), and the red fluorescence from rhodamine B (B,E) were detected on the cytoplasm of most cells, suggesting that the tbFGF fragment conjugated micelles could rapidly bind to the tumor cells that expressed FGFRs, aggregate around the cells and then release rhodamine B into the cytoplasm. More importantly, Fig. 7 also shows the fluorescent signal uptaken by A549 cells that overexpressed FGFRs was stronger than that uptaken by C26 cells which low expressed FGFRs. In accordance with the flow cytometry study, these results suggest that the cellular uptake of the functional micelles are mostly induced by the recognition and binding of the tbFGF fragments to the FGFRs that expressed on the surfaces of tumor cells.

## 4. Discussion

Nanoscopic therapeutic systems that incorporate therapeutic agents, molecular targeting and diagnostic imaging capabilities are emerging as the next generation of multifunctional nanomedicine

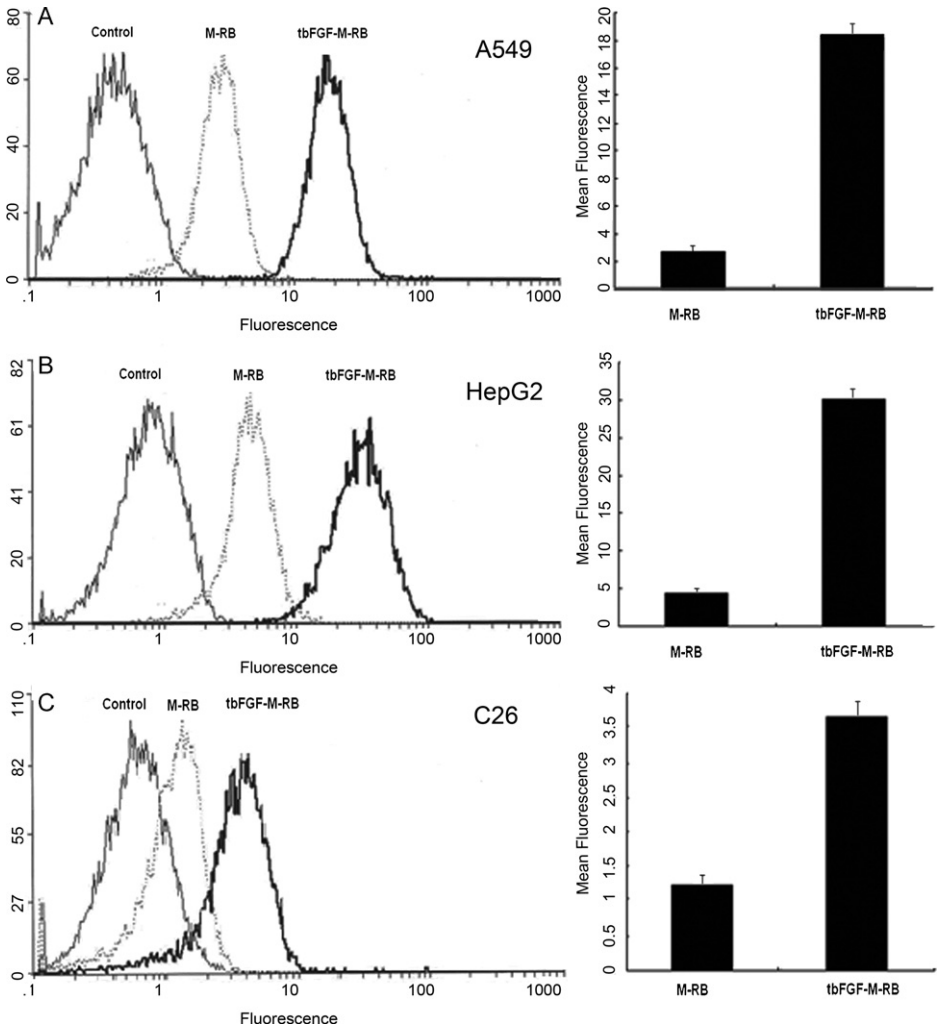


**Fig. 6.** Different cellular uptake of rhodamine B loaded micelles with or without tbFGF by A549, HepG2 and C26 cells. Panel A: Flow cytometry profiles (left) and quantification (right) of the mean fluorescence intensities of A549 cells after incubated with M-RB or tbFGF-M-RB, respectively; Panel B: Flow cytometry profiles (left) and quantification (right) of the mean fluorescence intensities of HepG2 cells after incubated with M-RB or tbFGF-M-RB, respectively; Panel C: Flow cytometry profiles (left) and quantification (right) of the mean fluorescence intensities of C26 cells after incubated with M-RB or tbFGF-M-RB, respectively. Error bars correspond to 95% confidence intervals. $P < 0.05$.

to improve the therapeutic outcome of drug therapy. Polymeric self-assembled nanoparticles from amphiphilic block polymers, provide a unique core-shell architecture, wherein the hydrophobic core serves as natural carrier environment for hydrophobic drugs and the hydrophilic shell allows particle stabilization in aqueous solution (Kwon, 2003; Otsuka et al., 2003; Torchilin, 2001). Sterically stabilized micelles by the PEG corona have shown prolonged blood circulation and "passive" tumor targeting effect through the enhanced permeability and retention (EPR) effect, leading to Phase III or II clinical trials of several micellar systems in cancer patients (Matsumura et al., 2004; Matsumura and Kataoka, 2009; Shuai et al., 2004). Nanoparticler size and prolonged circulation time are critical to the success of these therapeutic systems. The problem with these systems, however, is that the PEG-nanoparticles do not bind well to target cells at accumulation sites. The majority of these nanoparticles are still cleared by the RES system, resulting in short half lives and unwanted micelle deposition in the liver and spleen. To achieve ideal targeting for the most specific therapeutic effects, three factors, the accumulation of nanoparticles at disease sites, target cell-specific binding, and the delivery of drugs into target cells, have been undergoing (Bikram et al., 2004; Sutton et al., 2007).

Some studies revealed neutral or negative charged nanoparticles could have much longer circulation times in blood for their weaker interaction with serum proteins compared to positive charged nanoparticles (Moghimi et al., 2001). The tbFGF contains many basic amino residues, which may result in positive charge on the micelle surface. The positive charge may induce rapid uptake by RES and non-specific binding with unexpected cells, such as erythrocytes, after intravenous administration. To overcome this problem, we chosed the Chol-$PEG_{2000}$-COOH as the primary element of the micelles to get the negative micelle surfaces, which could enable paclitaxel to have prolonged circulation time in blood and improve its penetration and accumulation at tumor sites. Furthermore, the PEG chains were expected to limit the interactions with RES and other non-target cells. The *in vivo* antitumor study of the tbFGF-M-PTX and investigation in clear mechanistic understanding of how tbFGF conjugated Chol-PEG2000-COOH micelles affect tumor site targeting and tissue distribution will be our future work.

In the past decade, various functional polymeric micelles have been developed as targeting carriers for antitumor drugs, and there are several reports of clinical use of targeting micelles loaded with drugs such as doxorubicin or taxol (Matsumura et al., 2004; Moghimi et al., 2001; Nasongkla et al., 2006; Terada et al., 2007; Torchilin, 2001). The greatest challenges encountered in these attempts to use surface-modified micelles as drug carriers were decreased cytotoxicity against tumor cells compared with the free drugs (Hamaguchi et al., 2005; Kim et al., 2004; Nishiyama et al.,

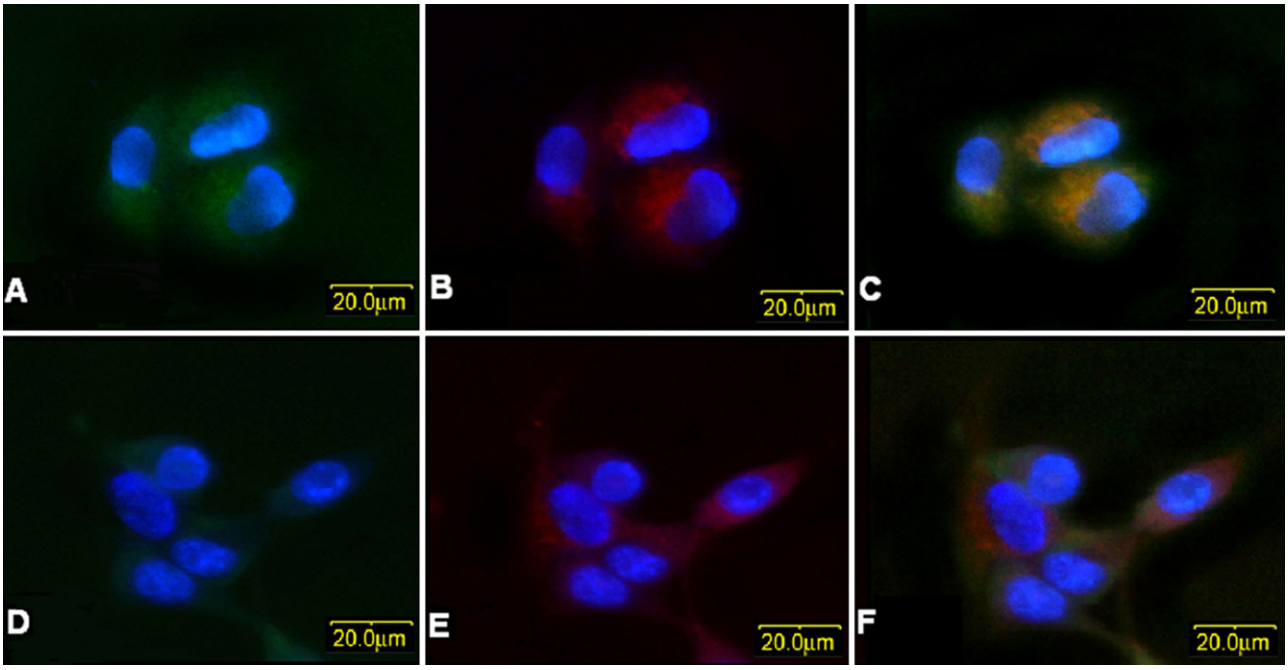


**Fig. 7.** The triple fluorescence-labeling microscopy images of A549 cells (A–C) and C26 cells (D–F) after incubation with rhodamine B-loaded Chol-$PEG_{2000}$-COOH micelles that were conjugated with the tbFGF fragments pre- labeled by FLUOS: green fluorescein images from the tbFGF fragments on the surface of tumor cells (A and D); red rhodamine B images around the blue Hoechst 33258-labeled nuclei (B, E); Overlay of green tbFGF and red rhodamine B images (C, F). (A) to (F) are magnified equally. Bar in (A): 20.0 μm. (For interpretation of the references to colour in this figure legend, the reader is referred to the web version of the article.)

2003) and inadequate stability of the integration between the micelles and the functional groups(Plum et al., 2000; Toncheva et al., 2003). Because of the decreased cytotoxicity, a high dose of drug in the micelles was used in clinic (Kim et al., 2004), resulting in problems of drug accumulation in other tissues and effects on metabolism. In comparison with other targeted drug delivery systems based on micelles, the great benefit of the tbFGF conjugated Chol-$PEG_{2000}$-COOH micellar system is that the tbFGF-M-PTX showed stronger cytotoxicity against tumor cells in *vitro* compared with the same dose of free PTX (Fig. 3C), which could be explained by the two mechanisms below: firstly the tbFGF fragments chemically conjugated on the surfaces of micelles enabled the PTX-loaded micelles to effectively target to the surfaces of LL/2 cells, which was confirmed by the flow cytometry study(Fig. 4) and the fluorescence microscopy image(Fig. 5); secondly the Chol-$PEG_{2000}$-COOH micellar drug delivery system increased solubility of the poorly soluble drugs in micelle solution, persistently released the drugs (Fig. 3B) and enhanced endocytotic uptake of drug-containing micelles. The slightly increase of cytotoxicity of M-PTX compared with free PTX is probably due to the Chol-$PEG_{2000}$-COOH polymer micellar drug delivery system increases the solubility of PTX and enhances the endocytotic uptake of PTX.

It has been reported that the FGF-2 of murine and human are high homologous (95%) (Plum et al., 2000). Moreover, the sequences of tbFGF fragments used in present investigation were approximately 98% similar to those in murine (He et al., 2003). In our study, both in human tumor cell lines (A549 and HepG2) and in murine tumor cell lines(LL/2 and C26), tbFGF-M-PTX exhibited more effective than M-PTX as a targeted drug delivery system *in vitro*(Figs. 4–6) which indicated that tbFGF peptides play an important role in the enhancement of specific uptake of drug by cells that overexpress FGFRs. The mean fluorescence intensities of A549 and HepG2 cells that overexpress FGFRs were higher than that of the C26 cells that low expressed FGFRs after incubated with tbFGF-M-RB(Fig. 6), and the fluorescent signal uptaken by the A549 cells was stronger than that by C26 cells(Fig. 7), suggesting that the tbFGF-M-PTX could specifically target to FGFR-overexpressing tumor cells. Therefore, further investigation of this strategy need to be done to provide us more information about the potential application to tumor targeting therapy in humans.

## 5. Conclusion

In conclusion, biologically active tumor targeting polymer core/shell micelles, the surfaces of which are anchored with truncated bFGF, have been successfully developed for drug delivery to the tumor cells. Poorly soluble antitumor drug paclitaxel as model is loaded into the micelles. The micelles are spheroids with regular shape, have a size distribution of about 10–50 nm and slightly negative surface charge. Flow cytometry results and fluorescence spectroscopy images suggest the presence of tbFGF on the surfaces of the micelles promot their uptakes by various tumor cells that express FGFRs. Thus the paclitaxel loaded-tbFGF fragment conjugated micelles have significantly enhanced cytotoxicity of paclitaxel for murine Lewis lung carcinoma cells, which was confirmed by MTT experiment. Although further investigation on the *in vivo* antitumor effect of tbFGF conjugated Chol-$PEG_{2000}$-COOH micelles is required, the findings of our study represent an important step in advancing the use of tbFGF conjugated Chol-$PEG_{2000}$-COOH micelles as a potent strategy to treat tumors that overexpress FGFRs.

## Acknowledgements

This work was supported by National Key Technologies R&D Program (2009ZX09501-015), National Natural Science Foundation of China (81071251) and the Open Research Fund of State Key Laboratory Breeding Base of Systematic Research, Development and Utilization of Chinese Medicine. We acknowledge Yongqiu Mao for her help in flow cytometry study, Chengjian Zhao for his help in fluorescence microscopy image study and Hailong Zhang for his help in RT-PCR study.

## References


Bikram, M., Ahn, C., Chae, S.Y., Lee, M., Yockman, J.W., Kim, S.W., 2004. Biodegradable poly (ethylene glycol)-co-poly (L-lysine)-g-histidine multiblock copolymers for nonviral gene delivery. Macromolecules 37, 1903–1916.

Chen, X., Wang, X.H., Wang, Y.S., Yang, L., Hu, J., Xiao, W.J., Fu, A.F., Cai, L.L., Li, X., Ye, X., Liu, Y.L., Wu, W.S., Shao, X.M., Mao, Y.Q., Wei, Y.Q., Chen, L.J., 2010. Improved tumor-targeting drug delivery and therapeutic efficacy by cationic liposome modified with truncated bFGF peptide. J. Control. Release 145, 17–25.

Dharap, S.S., Wang, Y., Chandna, P., Khandare, J.J., Qiu, B., Gunaseelan, S., Sinko, P.J., Stein, S., Farmanfarmaian, A., Minko, T., 2005. Tumor-specific targeting of an anticancer drug delivery system by LHRH peptide. Proc. Natl. Acad. Sci. U.S.A. 102, 12962–12967.

Goldman, C.K., Rogers, B.E., Douglas, J.T., Sosnowski, B.A., Ying, W.B., Siegal, G.P., 1997. Targeted gene delivery to Kaposi's sarcoma cells via the fibroblast growth factor receptor. Cancer Res. 57, 1447–1451.

Hamaguchi, T., Matsumura, Y., Suzuki, M., Shimizu, K., Goda, R., Nakamura, I., Nakatomi, I., Yokoyama, M., Kataoka, K., Kakizoe, T., 2005. NK105, a paclitaxel-incorporating micellar nanoparticle formulation, can extend in vivo antitumour activity and reduce the neurotoxicity of paclitaxel. Br. J. Cancer 92, 1240–1246.

Harashima, H., Ishida, T., Kamiya, H., Kiwada, H., 2002. Pharmacokinetics of targeting with liposomes. Crit. Rev. Ther. Drug Carrier Syst. 9, 235–275.

He, Q.M., Wei, Y.Q., Tian, L., Zhao, X., Su, J.M., Yang, L., Lu, Y., Kan, B., Lou, Y.Y., Huang, M.J., Xiao, F., Liu, J.Y., Hu, B., Luo, F., Jiang, Y., Wen, Y.j., Deng, H.X., Li, J., Niu, T., Yang, J.L., 2003. Inhibition of tumor growth with a vaccine based on xenogeneic homologous fibroblast growth factor receptor-1 in mice. Biol. Chem. 278, 21831–21836.

Kerbel, R.S., 2000. Tumor angiogenesis: past, present and the near future. Carcinogenesis 21, 505–515.

Kim, T.Y., Kim, D.W., Chung, J.Y., Shin, S.G., Kim, S.C., Heo, D.S., Heo, N.K., Bang, Y.J., 2004. Phase I and pharmacokinetic study of Genexol-PM, a cremophor-free, polymeric micelle-formulated paclitaxel, in patients with advanced malignancies. Clin. Cancer Res. 10, 3708–3716.

Kong, H.L., Crystal, R.G., 1998. Gene therapy strategies for tumor antiangiogenesis. J. Natl. Cancer Inst. 90, 273–286.

Kwon, G.S., 2003. Polymeric micelles for delivery of poorly water-soluble compounds. Crit. Rev. Ther. Drug Carrier Syst. 20, 357–403.

Lasic, D.D., 1992. Mixed micelles in drug delivery. Nature 355, 279–280.

Lee, H., Hu, M., Reilly, R.M., Allen, C., 2007. Apoptotic epidermal growth factor (EGF)-conjugated block copolymer micelles as a nanotechnology platform for targeted combination therapy. Mol. Pharm. 4, 769–781.

Li, D., Yu, H., Huang, H.L., Shen, F.P., Wu, X.Y., Li, J.Z., 2007. FGF receptor-mediated gene delivery using ligands coupled to Polyethylenimine. Biomater. Appl. 22, 163–180.

Liu, L.H., Guo, K., Lu, J., Venkatraman, S.S., Luo, D., Ng, K.C., Ling, E.A., Moochhala, S., Yang, Y.Y., 2008. Biologically active core/shell nanoparticles self-assembled from cholesterol-terminated PEG-TAT for drug delivery across the blood brain barrier. Biomaterials 29, 1509–1517.

Matsumura, Y., Hamaguchi, T., Ura, T., Muro, K., Yamada, Y., Shimada, Y., Shirao, K., Okusaka, T., Ueno, H., Ikeda, M., Watanabe, N., 2004. Phase I clinical trial and pharmacokinetic evaluation of NK911, a micelle-encapsulated doxorubicin. Br. J. Cancer 91, 1775–1811.

Matsumura, Y., Kataoka, K., 2009. Preclinical and clinical studies of anticancer agent-incorporating polymer micelles. Cancer Sci. 100, 572–579.

Moghimi, S.M., Hunter, A.C., Murray, J.C., 2001. Long-circulating and target-specific nanoparticles: theory to practice. Pharmacol. Rev. 53, 283–318.

Nasongkla, N., Bey, E., Ren, J., Ai, H., Khemtong, C., Setti Guthi, J., Chin, S.F., Sherry, A.D., Boothman, D.A., Gao, J., 2006. Multifunctional polymeric micelles as cancer-targeted, MRI-ultrasensitive drug delivery systems. Nano Lett. 6, 2427–2430.

Nishiyama, N., Okazaki, S., Cabral, H., Miyamoto, M., Kato, Y., Sugiyama, Y., Nishio, K., Matsumura, Y., Kataoka, K., 2003. Novel cisplatin-incorporated polymeric micelles can eradicate solid tumors in mice. Cancer Res. 63, 8977–8983.

Otsuka, H., Nagasaki, Y., Kataoka, K., 2003. PEGylated nanoparticles for biological and pharmaceutical applications. Adv. Drug Deliv. Rev. 5, 403–419.

Plum, S.M., Holaday, J.W., Ruiz, A., Madsen, J.W., Fogler, W.E., Fortier, A.H., 2000. Administration of a liposomal FGF-2 peptide vaccine leads to abrogation of FGF-2-mediated angiogenesis and tumor development. Vaccine 19, 1294–1303.

Rancourt, C., Rogers, B.E., Sosnowski, B.A., Wang, M.H., Piche, A., Pierce, G.F., 1998. Basic fibroblast growth factor enhancement of adenovirus-mediated delivery of the herpes simplex virus thymidine kinase gene results in augmented therapeutic benefit in a murine model of ovarian cancer. Clin. Cancer Res. 4, 2455–2461.

Rosa, P.A.J., Azevedo, A.M., Ferreira, I.F., Vries, J.de, Korporaal, R., Verhoef, H.J., Visser, T.J., 2007. J. Chromatogr. 1162, 103–113.

Shchors, K., Evan, G., 2007. Tumor angiogenesis: cause or consequence of cancer? Cancer Res. 67, 7059–7061.

Shuai, X., Ai, H., Nasongkla, N., Kim, S., Gao, J., 2004. Micellar carriers based on block copolymers of poly (epsilon-caprolactone) and poly (ethylene glycol) for doxorubicin delivery. J. Control. Release 98, 415–426.

Sosnowski, B.A., Gonzalez, A.M., Chandler, L.A., Buechler, Y.J., Pierce, G.F., Baird, A., 1996. Targeting DNA to cells with basic fibroblast growth factor (FGF2). J. Biol. Chem. 271, 33647–33653.

Sutton, D., Nasongk, N., Blanco, E., Gao, J., 2007. Functionalized micellar systems for cancer targeted drug delivery. Pharm. Res. 24, 1029–1046.

Terada, T., Mizobata, M., Kawakami, S., Yabe, Y., Yamashita, F., Hashida, M., 2006. Basic fibroblast growth factor-binding peptide as a novel targeting ligand of drug carrier to tumor cells. J. Drug Target 14, 536–545.

Terada, T., Mizobata, M., Kawakami, S., Yamashita, F., Hashida, M., 2007. Optimization of tumor-selective targeting by basic fibroblast growth factor-binding peptide grafted PEGylated liposomes. J. Control. Release 119, 262–270.

Toncheva, V., Schacht, E., Ng, S.Y., Barr, J., Heller, J., 2003. Use of block copolymers of poly (ortho esters) and poly (ethylene glycol) micellar carriers as potential tumour targeting systems. J. Drug Target. 11, 345–353.

Torchilin, V.P., 2001. Structure and design of polymeric surfactant-based drug delivery systems. J. Control. Release 73, 137–172.

Torchilin, P.V., Lukyanov, N.A., Gao, Z.G., Brigitte, P.S., 2003. Immunomicelles: Targeted pharmaceutical carriers for poorly soluble drugs. Proc. Natl. Acad. Sci. U.S.A. 100, 6039–6044.

Yamamoto, Y., Nagasaki, Y., Kato, Y., Sugiyama, Y., Kataoka, K., 2001. Long-circulating poly (ethylene glycol)-poly ($_{D,\ L}$-lactide) block copolymer micelles with modulated surface charge. J. Control. Release 77, 27–38.

Zamboni, W.C., 2005. Liposomal, nanoparticle, and conjugated formulations of anticancer agents. Clin. Cancer Res. 11, 8230–8234.

Zelphati, O., Wang, Y., Kitada, S., Reed, J.C., Felgner, P.L., Corbeil, J., 2001. Intracellular delivery of proteins with a new lipid-mediated delivery system. J. Biol. Chem. 276, 35103–35110.